2

Mathematical Modeling

2.1 GENERALIZED SYSTEM PROPERTIES

In this chapter, we will review the basic concepts and methods employed in the development of "gray-box" models. Models of very different systems often contain properties that can be characterized using the same mathematical expression. The first of these is the *resistive* property. Everyone is familiar with the concept of electrical resistance (R), which is defined by Ohm's law as

$$V = RI \tag{2.1}$$

where V is the voltage or driving potential across the resistor and I represents the current that flows through it. Note that V is an "across" variable and may be viewed as a measure of "effort," I, on the other hand, is a "through" variable and represents a measure of "flow." Thus, if we define the generalized "effort" variable, ψ, and the generalized "flow" variable, ζ, Ohm's law becomes:

$$\psi = R\zeta \tag{2.2}$$

where R now represents a generalized resistance. Figure 2.1 shows the application of this concept of generalized resistance to different kinds of systems. In the mechanical dashpot, when a force F is applied to the plunger (and, of course, an equal and opposite force is applied to the dashpot casing), it will move with a velocity v that is proportional to F. As illustrated in Figure 2.1a, this relationship takes on the same form as the generalized Ohm's law (Equation (2.2)), when F and v are made to correspond to ψ and ζ, respectively. The constant of proportionality, R_m, which is related to the viscosity of the fluid inside the dashpot, provides a measure of "mechanical resistance." In fact, R_m determines the performance of the dashpot as a shock absorber and is more commonly known as the "damping coefficient." In fluid flow, the generalized Ohm's law assumes the form of Poiseuille's law, which states that the volumetric flow of fluid (Q) through a rigid tube is proportional to the pressure difference (ΔP) across the two ends of the tube. This is illustrated

in Figure 2.1b. Poiseuille further showed that the fluid resistance, R_f, is directly related to the viscosity of the fluid and the length of the tube, and inversely proportional to the square of the tube cross-sectional area. In Fourier's law of thermal transfer, the flow of heat, Q, conducted through a given material is directly proportional to the temperature difference that exists across the material (Figure 2.1c). Thermal resistance, R_t, can be shown to be inversely related to the thermal conductivity of the material. Finally, in chemical systems, the flux, Q, of a given chemical species across a permeable membrane separating two fluids with different species concentrations is proportional to the concentration difference, $\Delta\phi$ (Figure 2.1d). This is known as Fick's law of diffusion. The diffusion resistance, R_c, is inversely proportional to the more commonly used parameter, the membrane diffusivity.

The second generalized system property is that of *storage*. In electrical systems, this takes the form of capacitance, defined as the amount of electrical charge (q) stored in the capacitor per unit voltage (V) that exists across the capacitor:

$$C = \frac{q}{V} \tag{2.3}$$

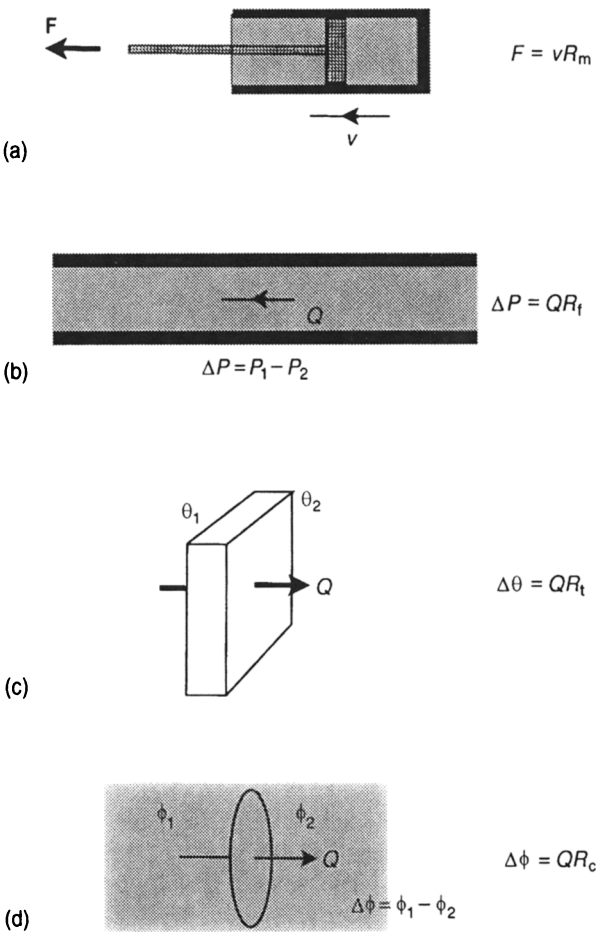

Figure 2.1 "Resistance" in (a) mechanical, (b) fluidic, (c) thermal, and (d) chemical systems.

Note that q represents the accumulation of all electric charge delivered via current flow to the capacitor, so that the following relationship exists between q and I:

$$q = \int_0^t I\, dt \tag{2.4}$$

Thus, using Equation (2.4) in Equation (2.3) and rewriting the result in generalized form, we obtain the following expression:

$$\psi = \frac{1}{C}\int_0^t \zeta\, dt \tag{2.5}$$

For mechanical systems, this storage property takes the form of "compliance," as in the case of the elastic spring shown in Figure 2.2a. For a given applied force, the mechanical compliance determines the extent to which the spring will be extended or compressed. This property is also inversely related to the stiffness or elastic modulus of the spring: the more compliant the spring, the less stiff it will be, and the more it will extend for a given applied tension. Similarly, in fluidic systems, as represented in the example of the fluid-filled balloon in Figure 2.2b, compliance determines the volume by which the balloon will expand or contract per unit change in applied pressure. The compliance here is determined primarily by the elasticity of the balloon material: the stiffer the material, the less "compliant" the balloon. A much smaller contribution to the compliance arises from the compressibility of the fluid inside the balloon. In thermal systems, the "thermal mass" represents the amount of heat stored in a certain medium per unit difference in temperature that exists between the interior and exterior (Figure 2.2c). This thermal capacitance depends on the dimensions and specific heat of the medium in question. Finally, in chemical systems, the storage property is

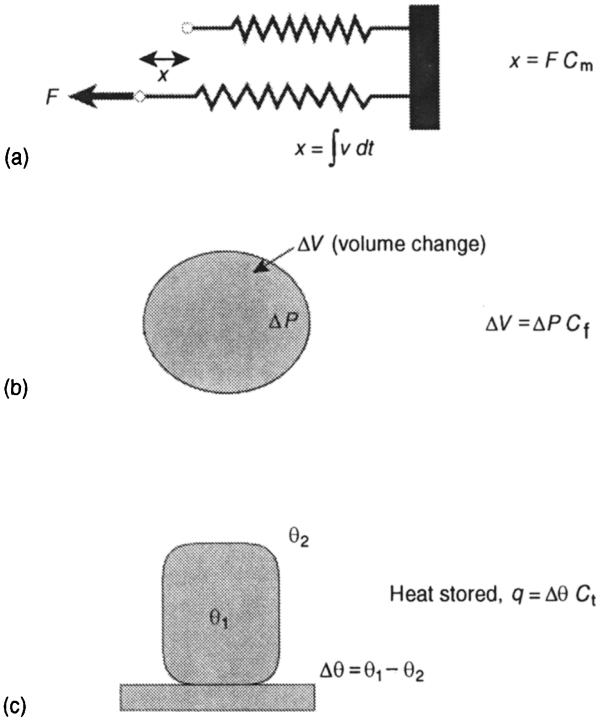

Figure 2.2 "Capacitance in (a) mechanical, (b) fluidic, (c) thermal, and (d) chemical systems.

represented by the total volume of the fluid in which the chemical species exists (Figure 2.2d), i.e., for given volume, the total mass of the chemical species present is proportional to its concentration. This property, in fact, is used in the *definition* of concentration.

The resistive and storage properties also represent elements through which energy is dissipated or stored, respectively. In the context of electrical resistance, note that the product of voltage and current yields power. In mechanical systems, force multiplied by velocity also yields power. Similarly, in fluidic systems, power is defined as the product of pressure and flow rate. Thus, in any general system, energy is *dissipated* when effort is applied to produce flow through the resistive element. On the other hand, the storage element allows the accumulation of "static" or *potential energy*. For instance, in the mechanical spring, application of force F which produces an extension of x length units will lead to the storage of Fx units of potential energy. Similarly, in the balloon system, potential energy is stored when the balloon is expanded with the application of internal pressure.

The final generalized system property, *inertance*, allows the storage of *kinetic energy* in electrical systems. This property is also known as *inductance* (L), which is defined as the voltage required to produce a given rate of change of electrical current:

$$V = L \frac{dI}{dt} \tag{2.6}$$

Replacing V and I by the corresponding generalized system variables, ψ and ζ, we have:

$$\psi = L \frac{d\zeta}{dt} \tag{2.7}$$

Note that in the context of mechanical systems, ψ becomes F (force) and ζ becomes velocity, so that Equation (2.7) becomes Newton's Second Law of Motion: force equals mass times acceleration. Thus, in this case, the inertance is simply the mass of the system. Inertance is also present in fluidic systems, so that fluid acceleration is proportional to the pressure differential applied. On the other hand, there is no element that represents inertance in thermal and chemical systems; kinetic energy storage does not exist in these systems.

2.2 MODELS WITH COMBINATIONS OF SYSTEM ELEMENTS

An assumption implicit in the previous section is that the system properties are time-invariant and independent of the values of the generalized system variables. In other words, the three basic model elements are *linear*. In reality, this will not be the case. An electrical resistor will heat up as the current that passes through it increases, thereby raising its resistance. Similarly, fluid resistance remains relatively constant only under conditions of steady, laminar flow; as flow increases and becomes turbulent, the resistance becomes a function of flow itself. Thus, as the effect of nonlinearities increases, the similarities in behavior among these different systems will be progressively reduced. Nevertheless, in scientific exploration, we always have to start somewhere—and past scientific history has shown that it is wise to begin with the simplest model. Therefore, linear analysis plays an important role in physiological systems modeling by allowing us to obtain a first approximation to the underlying reality.

We will proceed with our discussion of linear analysis by considering how we can derive the overall model equations from various combinations of the three basic types of system elements. Figure 2.3 shows a simple "circuit" linking three generalized system elements in series and parallel. The node labeled "0" represents the reference level of the "effort" variable ψ to which all other nodes are compared; this is set equal to zero. In

electrical systems, this node would be called "electrical ground." ψ_a and ψ_c represent the values of the *across-variables* at nodes a and b, respectively, relative to node 0. ζ_1, ζ_2 and ζ_3 represent the values of the *through-variables* that pass through the elements E1, E2, and E3, respectively. The mathematical relationships among these variables can be derived by applying two fundamental physical principles:

1. The algebraic sum of the "across-variable" values around any closed circuit must equal zero. Thus, in the loop a–b–0–a in Figure 2.3, we have

$$(\psi_a - \psi_b) + (\psi_b - 0) + (0 - \psi_a) = 0 \tag{2.8}$$

2. The algebraic sum of all "through-variable" values into a given node must equal zero. In Figure 2.3, the only node where this rule will apply is node b:

$$\zeta_1 + (-\zeta_2) + (-\zeta_3) = 0 \tag{2.9}$$

The preceding two generalized principles take the form of Kirchhoff's laws when applied to electrical systems. The first (voltage) law appears trivial in the form presented, but in order to apply this law, each of the component terms in the left-hand side of Equation (2.8) has to be expressed as a function of the corresponding through-variables and the system elements. The second (current) law is essentially a statement of the conservation of mass principle. In Equation (2.9), ζ_2 and ζ_3 are given negative signs since, in Figure 2.3, they assume a flow direction that points away from node b. Although each of the boxes labeled E1, E2, and E3 was intended to represent one of the three basic system elements, each in general could also contain a network within itself; within each network, the above two laws would still apply. Thus, starting from the basic system elements, we can construct progressively more complex models by connecting these elements in either series or parallel configurations. And by using the generalized Kirchhoff's laws, it is possible to deduce mathematical expressions that characterize the overall properties of these synthesized networks. Figure 2.4 illustrates the resultant system properties that emerge from simple combinations of resistive and storage elements for electrical, fluidic, thermal, and chemical systems. These results are easily derived using basic circuit analysis.

The expressions that relate combined resistances and compliances to their respective component elements are somewhat different for mechanical systems, as Figure 2.5 shows. Consider case (a), where the two mechanical dashpots (resistances) are placed in parallel. This parallel configuration constrains the motion of the two dashpot plungers by requiring them to

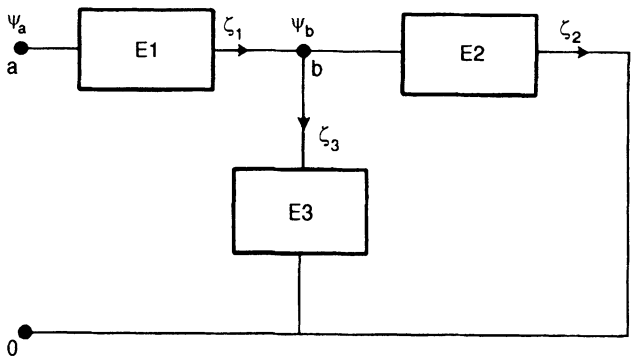

Figure 2.3 Simple model consisting of a network of generalized system elements.

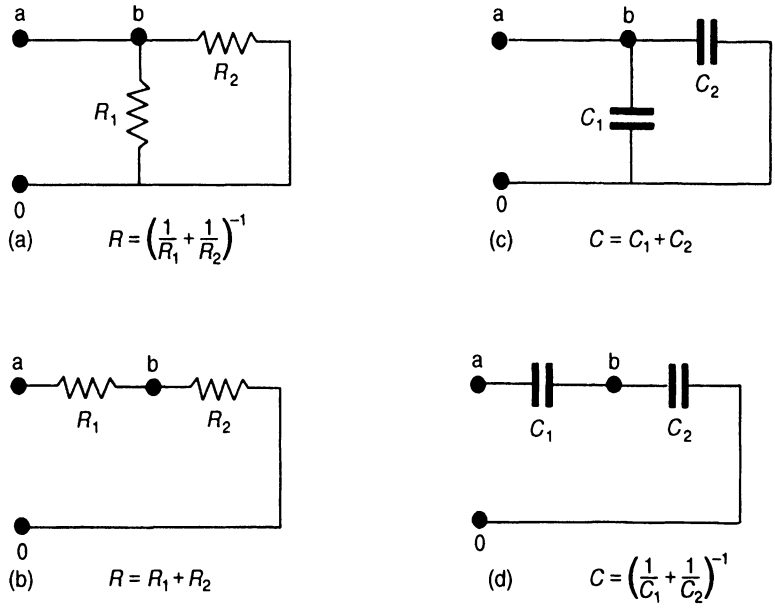

Figure 2.4 Model properties that emerge from simple networks of system elements in electrical, fluidic, thermal, and chemical systems.

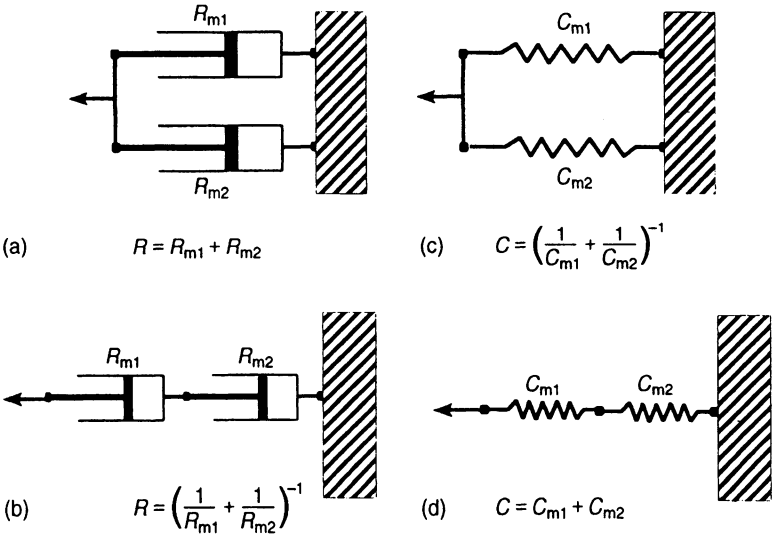

Figure 2.5 Models of parallel and series combinations of mechanical dashpots (resistances) and springs (compliances).

move at the same velocity. Therefore, the total force F required to extend the two dashpots with resistances R_{m1} and R_{m2} at velocity v is

$$F = v(R_{m1} + R_{m2}) \tag{2.10}$$

But the combined resistance, R, is defined as F/v. Thus, Equation (2.10) yields:

$$R = R_{m1} + R_{m2} \tag{2.11}$$

This relationship for the two mechanical resistances in parallel is different from the corresponding expression for parallel combinations of the other types of resistances.

Case (c) in Figure 2.5 represents mechanical springs with compliances C_{m1} and C_{m2} connected in parallel. As in case (a), the parallel mechanical arrangement constrains the springs so that they must extend by equal amounts ($=x$). Thus,

$$x = F_1 C_{m1} = F_2 C_{m2} \tag{2.12}$$

where F_1 and F_2 represent the corresponding tensions developed in the two springs. But the sum of F_1 and F_2 yields the total force F required to extend the spring combination by x, and since $C = x/F$ by definition, Equation (2.12) leads to

$$\frac{1}{C} = \frac{1}{C_{m1}} + \frac{1}{C_{m2}} \tag{2.13}$$

which again differs from the corresponding situation for capacitances placed in parallel in other systems. Similar considerations apply to series combinations of mechanical dashpots and springs (cases (b) and (d) in Figure 2.5). As such, one has to be cautious in converting models of mechanical systems into their electrical analogs.

2.3 LINEAR MODELS OF PHYSIOLOGICAL SYSTEMS: TWO EXAMPLES

In this section, we will derive the mathematical formulations that characterize the input–output properties of two simple physiological models. The first model provides a linearized description of lung mechanics (Figure 2.6). The airways are divided into two categories: the larger or central airways and the smaller or peripheral airways, with fluid mechanical resistances equal to R_C and R_P, respectively. Air that enters the alveoli also produces an expansion of the chest-wall cavity by the same volume. This is represented by the connection of the lung (C_L) and chest-wall (C_W) compliances in series. However, a small fraction of the volume of air that enters the respiratory system is shunted away from the alveoli as a result of the compliance of the central airways and gas compressibility. This shunted volume is very small under normal circumstances at regular breathing frequencies, but becomes progressively more substantial if disease leads to peripheral airway obstruction (i.e., increased R_P) or a stiffening of the lungs or chest-wall (i.e., decreased C_L or C_W). We account for this effect by

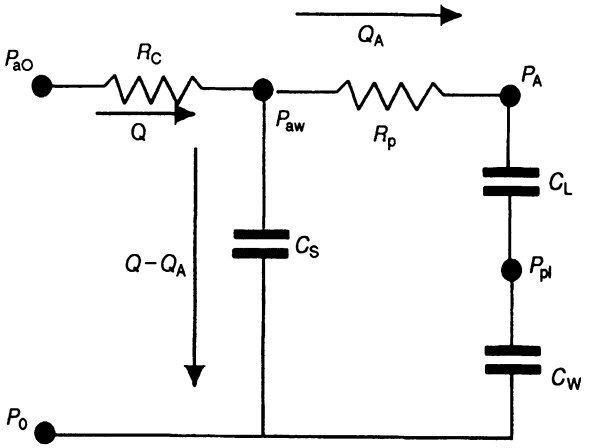

Figure 2.6 Linear model of respiratory mechanics.

placing a shunt compliance, C_S, in parallel with C_L and C_W. The pressures developed at the different points of this lung model are: P_{ao} at the airway opening, P_{aw} in the central airways, P_A in the alveoli and P_{pl} in the pleural space (between the lung parenchyma and chest wall). These pressures are referenced to P_0, the ambient pressure, which we can set to zero. Suppose the volume flow-rate of air entering the respiratory system is Q. Then, the objective here is to derive a mathematical relationship between P_{ao} and Q.

From Kirchhoff's Second Law (applied to the node P_{aw}), if the flow delivered to the alveoli is Q_A, then the flow shunted away from the alveoli must be $Q - Q_A$. Applying, Kirchhoff's First Law to the closed circuit containing C_S, R_P, C_L, and C_W, we have

$$R_P Q_A + \left(\frac{1}{C_L} + \frac{1}{C_W}\right)\int Q_A\, dt = \frac{1}{C_S}\int (Q - Q_A)\, dt \tag{2.14}$$

Applying Kirchhoff's First Law to the circuit containing R_C and C_S, we have

$$P_{ao} = R_C Q + \frac{1}{C_S}\int (Q - Q_A)\, dt \tag{2.15}$$

Differentiating Equation (2.14) and Equation (2.15) with respect to time, and subsequently reducing the two equations to one by eliminating Q_A, we obtain the equation relating P_{ao} to Q:

$$\frac{d^2P_{ao}}{dt^2} + \frac{1}{R_P C_T}\frac{dP_{ao}}{dt} = R_C\frac{d^2Q}{dt^2} + \left(\frac{1}{C_S} + \frac{R_C}{R_P C_T}\right)\frac{dQ}{dt} + \frac{1}{R_P C_S}\left(\frac{1}{C_L} + \frac{1}{C_W}\right)Q \tag{2.16}$$

where C_T is defined by

$$C_T = \left(\frac{1}{C_L} + \frac{1}{C_W} + \frac{1}{C_S}\right)^{-1} \tag{2.17}$$

The second example that we will consider is the linearized physiological model of skeletal muscle, as illustrated in Figure 2.7. F_0 represents the force developed by the active contractile element of the muscle, while F is the actual force that results after taking into account the mechanical properties of muscle. R represents the viscous damping inherent in the tissue, while C_P (parallel elastic element) and C_S (series elastic element) reflect the elastic

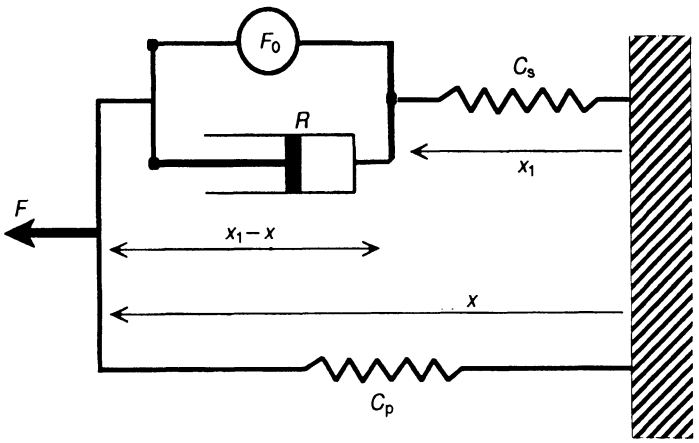

Figure 2.7 Linear model of muscle mechanics.

storage properties of the sarcolemma and the muscle tendons, respectively. First, consider the mechanical constraints placed on the model components as a result of the parallel configuration. If spring C_P is stretched by an incremental length x, the entire series combination of R and C_S will also extend by the same length. Furthermore, the sum of the force transmitted through the two branches of the parallel configuration must equal F. However, although the sum of the extensions of C_S and R will have to equal x, the individual length contributions from C_S and R need not be equal. Thus, if we assume C_S is stretched a length x_1, then the extension in the parallel combination of R and F_0 will be $x - x_1$. The velocity with which the dashpot represented by R is extending is obtained by differentiating $x - x_1$ with respect to time, i.e., $d(x - x_1)/dt$.

Using the principle that the force transmitted through C_S must be equal to the force transmitted through the parallel combination of F_0 and R, we obtain the following equation:

$$\frac{x_1}{C_S} = R\left(\frac{dx}{dt} - \frac{dx_1}{dt}\right) + F_0 \tag{2.18}$$

Then, using the second principle, i.e., that the total force from both limbs of the parallel combination must sum to F, we have

$$F = \frac{x_1}{C_S} + \frac{x}{C_P} \tag{2.19}$$

Eliminating x_1 from Equation (2.18) and Equation (2.19) yields the following differential equation relating F to x and F_0:

$$\frac{dF}{dt} + \frac{1}{RC_S}F = \left(\frac{1}{C_S} + \frac{1}{C_P}\right)\frac{dx}{dt} + \frac{1}{RC_SC_P}x + \frac{F_0}{RC_S} \tag{2.20}$$

Note that in Equation (2.20), under steady-state, isometric conditions (i.e., the muscle length is constrained to be constant), $x = 0$, $dx/dt = 0$ and $dF/dt = 0$, which leads to the result $F = F_0$. Therefore, under steady-state isometric conditions, the force developed by the muscle model will reflect the force developed by the active contractile element of the muscle.

2.4 DISTRIBUTED-PARAMETER VERSUS LUMPED-PARAMETER MODELS

The models that we have considered up to this point are known as *lumped-parameter models*. A given property of the model is assumed to be "concentrated" into a single element. For example, in the lung mechanics model (Figure 2.6), the total resistance of the central airways is "lumped" into a single quantity, R_C, even though in reality the central airways are comprised of the trachea and a few branching generations of airways, each of which has very different fluid mechanical resistance. Similarly, a single constant, C_L, is assumed to represent the compliance of the lungs, even though the elasticity of lung tissue varies from region to region. In order to provide a more realistic characterization of the *spatial* distribution of system properties, it is often useful to develop a *distributed-parameter model*. This kind of model generally takes the form of one or more partial differential equations with time and some measure of space (e.g., length or volume) as independent variables.

A distributed-parameter model can be viewed as a network of many infinitesimally small lumped-parameter submodels. To illustrate this relationship, we will derive the governing differential equation of a distributed-parameter model of the passive cable characteristics of an unmyelinated nerve fiber. As shown in Figure 2.8, the nerve fiber is

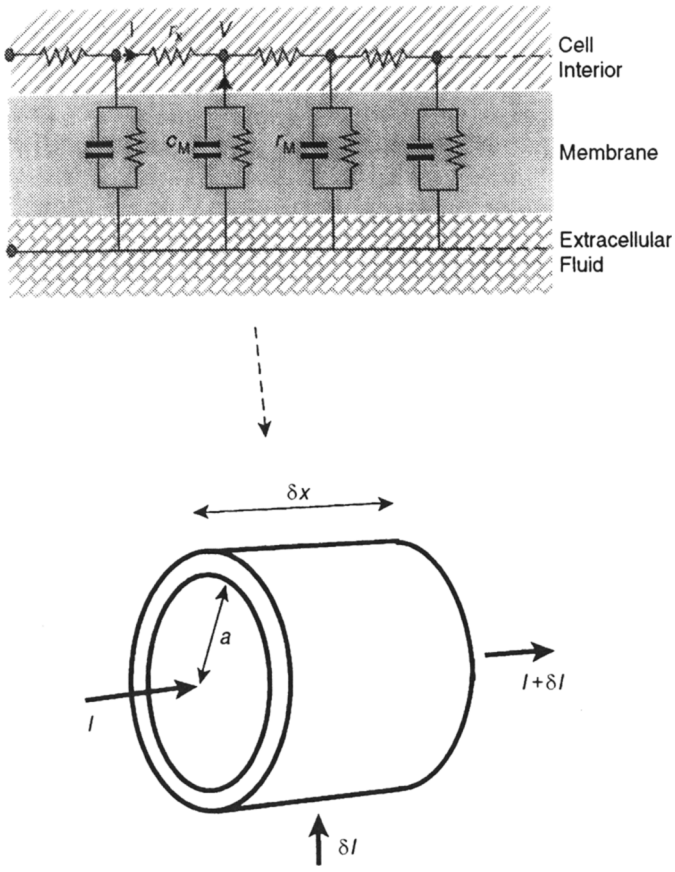

Figure 2.8 Relationship between the lumped-parameter and distributed-parameter models of the passive cable characteristics of an unmyelinated nerve fiber.

modeled as a network containing serially-connected multiple subunits, each with circuit elements r_x, r_M and c_M. r_x represents the axial resistance of 1 cm of nerve tissue per cm^2 of cross-sectional area, and is given in Ω cm. r_M and c_M represent the resistance and capacitance of 1 cm^2 of nerve membrane surface area, respectively. We assume that the extracellular medium bathing the nerve fiber represents the electrical ground in this model. How do we relate the current passing through to the voltage found at any point in this "cable"?

In the distributed-parameter model, the nerve fiber takes the form of a long cylindrical conductor of radius a. We focus our analysis on a small length δx of this cable which contains one of these resistance–capacitance subunits. We assume the intracellular voltage to increase by δV and the axial current to increase by δI over this small segment of cable. The assumption of "increases" instead of "decreases" in V and I merely establishes a sign convention. In reality, the voltage along the nerve fiber drops as current flows out of the nerve fiber through a leaky membrane. If we adopt the stated sign convention in a consistent manner, the final results will show the change in V or I with length to be negative. The voltage increase δV occurring over an axial distance of δx is related to the axial current by

$$\delta V = -\frac{I r_x \, \delta x}{\pi a^2} \tag{2.21}$$

The right-hand side of Equation (2.21) bears a negative sign since the "increase" in voltage should be associated with a current flowing in a direction *opposite* to that assumed in the figure. Dividing both sides of Equation (2.21) by δx, and taking the limit as δx is made to approach zero, we obtain

$$\frac{\partial V}{\partial x} = -\frac{Ir_x}{\pi a^2} \tag{2.22}$$

The membrane current, δI, is related to the intracellular voltage V by

$$\delta I = -\left(\frac{V}{r_M} 2\pi a\, \delta x + c_M\, 2\pi a\, \delta x \frac{\partial V}{\partial t}\right) \tag{2.23}$$

Again, dividing both sides of Equation (2.23) by δx and taking the limit as δx approaches zero, we obtain

$$\frac{\partial I}{\partial x} = -\left(\frac{V}{r_M} 2\pi a + c_M\, 2\pi a \frac{\partial V}{\partial t}\right) \tag{2.24}$$

Finally, Equation (2.22) and Equation (2.24) can be combined into one equation by differentiating Equation (2.22) with respect to x and substituting for $\partial I/\partial x$ in Equation (2.24):

$$\frac{\partial^2 V}{\partial x^2} = \frac{2r_x}{a}\left(c_M \frac{\partial V}{\partial t} + \frac{V}{r_M}\right) \tag{2.25}$$

Equation (2.25) is known as the one-dimensional cable equation, and describes intracellular voltage along the nerve fiber as a continuous function of length and time.

2.5 LINEAR SYSTEMS AND THE SUPERPOSITION PRINCIPLE

All the models we have considered up to this point are *linear systems*. We have shown that these linear systems can be characterized by linear ordinary or partial differential equations. A differential equation is linear when all its terms that contain the output and input variables and its derivatives are of the first degree. For example, the model differential equations that we have derived are of the general form:

$$a_2 \frac{d^2y}{dt} + a_1 \frac{dy}{dt} + y = b_2 \frac{d^2x}{dt} + b_1 \frac{dx}{dt} + b_0 x \tag{2.26}$$

Since all terms in y and its derivatives, as well as all terms in x and its derivatives, are raised to only the first power (degree), Equation (2.26) is linear. If the coefficients a_1, a_2, b_0, b_1 and b_2 are constants, then Equation (2.26) is also *time-invariant*. On the other hand, if one or more of these coefficients are functions of time, for example, if $a_1 = t$, Equation (2.26) remains linear but becomes *time-varying*. However, if one or more of the coefficients are functions of y or x, Equation (2.26) becomes *nonlinear*.

Let us suppose that the input x of the system described by Equation (2.26) takes on a particular time-course, e.g., $x = x_1(t)$, and the resulting time-course for y is $y_1(t)$. Then it follows that

$$a_2 \frac{d^2y_1}{dt} + a_1 \frac{dy_1}{dt} + y_1 = b_2 \frac{d^2x_1}{dt} + b_1 \frac{dx_1}{dt} + b_0 x_1 \tag{2.27}$$

When x takes on a different time-course $x_2(t)$ and the resulting time-course for y is $y_2(t)$, the following relationship also holds:

$$a_2 \frac{d^2y_2}{dt} + a_1 \frac{dy_2}{dt} + y_2 = b_2 \frac{d^2x_2}{dt} + b_1 \frac{dx_2}{dt} + b_0x_2 \tag{2.28}$$

By adding terms on both sides of Equation (2.27) and Equation (2.28) with the same coefficients, we have

$$a_2 \frac{d^2(y_1 + y_2)}{dt} + a_1 \frac{d(y_1 + y_2)}{dt} + (y_1 + y_2) = b_2 \frac{d^2(x_1 + x_2)}{dt} + b_1 \frac{d(x_1 + x_2)}{dt} + b_0(x_1 + x_2) \tag{2.29}$$

What Equations (2.27) through (2.29) together imply is that the response of a linear system to the sum of two different inputs is equal to the sum of the responses of the system to the individual inputs. This result can be extended to more than two inputs and is known as the *principle of superposition*. It is a defining property of linear systems and is frequently used as a test to determine whether a given system is linear.

The principle of superposition also implies that the complete solution (i.e., response in y) to Equation (2.26) can be broken down into two components, i.e.,

$$y(t) = y_c(t) + y_p(t) \tag{2.30}$$

where $y_c(t)$ is known as the *complementary function* and $y_p(t)$ is called the *particular solution*. $y_c(t)$ is the response of the linear system in Equation (2.26) when the input forcing $x(t)$ is set equal to zero, i.e.,

$$a_2 \frac{d^2y_c}{dt} + a_1 \frac{dy_c}{dt} + y_c = 0 \tag{2.31}$$

Thus, $y_c(t)$ reflects the component of $y(t)$ that remains the same independently of the form of input $x(t)$. However, the time-course of $y_c(t)$ depends on the initial values taken by y and its derivatives immediately prior to input stimulation. On the other hand, $y_p(t)$ is the response of the same linear system when the input forcing $x(t)$ is a particular function of time. Thus, $y_p(t)$ satisfies the differential equation:

$$a_2 \frac{d^2y_p}{dt} + a_1 \frac{dy_p}{dt} + y_p = b_2 \frac{d^2x}{dt} + b_1 \frac{dx}{dt} + b_0x \tag{2.32}$$

Unlike $y_c(t)$, $y_p(t)$ depends only on the coefficients of Equation (2.32) and the time-course of the input $x(t)$. If the linear system in question is *stable*, then the component of $y(t)$ characterized by $y_c(t)$ will eventually decay to zero while the overall response of the system will be increasingly dominated by $y_p(t)$. For this reason, $y_c(t)$ is also called the *transient response*; $y_p(t)$ is known as the *steady-state response* when $x(t)$ is an input forcing function that persists over time.

2.6 LAPLACE TRANSFORMS AND TRANSFER FUNCTIONS

We have shown that linear systems analysis provides the tools that allow us to build increasingly more complex models from smaller and simpler structures that ultimately can be broken down into various combinations of the three basic types of system elements. At each hierarchical level, each structure can be described functionally by its input–output characteristics, which can be expressed mathematically in the form of a differential equation

relating the input, $x(t)$, to output, $y(t)$. We now introduce a means of linking the mathematical description of a given system with its block diagram representation.

The Laplace transformation, denoted by $\mathscr{L}[\cdot]$, and its inverse, denoted by $\mathscr{L}^{-1}[\cdot]$, are mathematical operations defined as follows:

$$\mathscr{L}[y(t)] \equiv Y(s) \equiv \int_0^\infty y(t)e^{-st}\,dt \tag{2.33a}$$

$$\mathscr{L}^{-1}[Y(s)] \equiv \frac{1}{2\pi j}\int_{\sigma-j\infty}^{\sigma+j\infty} Y(s)e^{st}\,ds \tag{2.33b}$$

where the Laplace variable s is complex, i.e., $s = \sigma + j\omega$, and $j = \sqrt{-1}$. By employing the mathematical operation defined in Equation (2.33a), the function of time, $y(t)$, is converted into an equivalent function, $Y(s)$, in the complex s-domain. If we apply this mathematical operation to the time-derivative of y, dy/dt, we can evaluate the result by performing an integration by parts procedure:

$$\mathscr{L}\left[\frac{dy(t)}{dt}\right] \equiv \int_0^\infty \frac{dy(t)}{dt}e^{-st}\,dt = s\int_0^\infty y(t)e^{-st}\,dt + \left[y(t)e^{-st}\right]_0^\infty \tag{2.34a}$$

Thus,

$$\mathscr{L}\left[\frac{dy}{dt}\right] = sY(s) - y(0) \tag{2.34b}$$

By applying the same transformation to d^2y/dt^2, it can be shown that

$$\mathscr{L}\left[\frac{d^2y}{dt^2}\right] = s^2Y(s) - sy(0) - \left(\frac{dy}{dt}\right)_{t=0} \tag{2.35}$$

Conversely, the Laplace transform of the time-integral of $y(t)$, assuming $y(t) = 0$ for $t < 0$, is

$$\mathscr{L}\left[\int_0^t y(t)\,dt\right] = \frac{Y(s)}{s} \tag{2.36}$$

If we apply the Laplace transformation to the linear system represented by Equation (2.26), and use the above expressions in Equation (2.34b) and Equation (2.35) to evaluate the transforms of the derivatives, we will obtain the following result:

$$a_2s^2Y(s) + a_1sY(s) + Y(s) = b_2s^2X(s) + b_1sX(s) + b_0X(s) \tag{2.37a}$$

Equation (2.37a) assumes that the values of x and y and their first time-derivatives are all equal zero at time $t = 0$. Even if any one of these initial values are actually nonzero, they do not affect the functional nature of the dynamics of the linear system being characterized. Equation (2.37a) can be rearranged and presented in the following form:

$$\frac{Y(s)}{X(s)} = \frac{b_2s^2 + b_1s + b_0}{a_2s^2 + a_1s + 1} \tag{2.37b}$$

Equation (2.37b) describes in very compact format how the input to the linear system in question is transformed into its output. For any given input $x(t)$, it is possible to compute its Laplace transform, $X(s)$. Then, multiplying $X(s)$ by the function displayed on the right-hand side of Equation (2.37b), we can obtain the Laplace transform, $Y(s)$, of the system response. Finally, by inverting the transform, we can recover the time-course of the response, $y(t)$. Of course, we could have derived $y(t)$ by solving the differential equation in Equation (2.26).

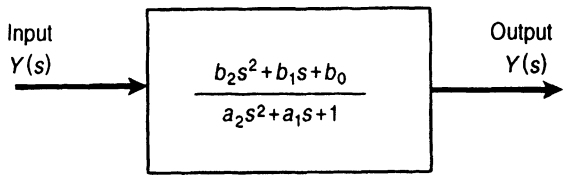

Figure 2.9 Transfer function representation of the linear system described by Equation (2.26)

However, application of the Laplace transformation converts the differential equation into an algebraic equation, which is generally easier to solve. The ratio of $Y(s)$ to $X(s)$ in Equation (2.37b) is called the *transfer function* of the system in question. Employing this approach allows the convenient representation of the input–output characteristics of any linear system in block diagram form, as illustrated in Figure 2.9 for the example that we have been discussing.

Laplace transforms of various "standard" functions in time have been evaluated and are available in the form of tables, such as that presented in Appendix I. These same tables are also used to convert Laplace expressions back into time-domain functions. One useful technique is to expand the transfer function into simpler partial fraction forms prior to performing the inverse Laplace transformation. For example, in Equation (2.37b), suppose $b_2 = 0$, $b_1 = 0.5$, $b_0 = 1.25$, $a_2 = 0.25$ and $a_1 = 1.25$. If the input were to take the form of a unit step (i.e., $x(t) = 1$ for $t > 0$ and $x(t) = 0$ for $t \leq 0$), then from Appendix I, $X(s) = 1/s$. Substituting these values into Equation (2.37b) would yield

$$Y(s) = \frac{0.5s + 1.25}{s(s+1)(0.25s+1)} = \left(\frac{1}{s} - \frac{1}{s+1}\right) + 0.25\left(\frac{1}{s} - \frac{1}{s+4}\right) \tag{2.38}$$

The time-course of the resulting output, $y(t)$, is obtained by performing the inverse Laplace transformation of the above partial fractions, using Appendix I:

$$y(t) = (1 - e^{-t}) + 0.25(1 - e^{-4t}) \tag{2.39}$$

More details on the methodological aspects of solving differential equations via Laplace transforms can be found in any standard text on applied mathematics or linear systems theory.

2.7 THE IMPULSE RESPONSE AND LINEAR CONVOLUTION

Suppose we have a linear system with unknown transfer function $H(s)$. Since, by definition, $Y(s) = H(s)X(s)$, if we can find an input $x(t)$ that has the Laplace transform $X(s) = 1$, then $Y(s) = H(s)$, i.e., the Laplace transform of the resulting response would reveal the transfer function of the unknown system. Appendix I shows that the time-function that corresponds to $X(s) = 1$ is $\delta(t)$, the Dirac delta function or the *unit impulse*. The unit impulse may be considered a rectangular pulse of infinite amplitude but infinitesimal duration. Consider the function $p(t)$ defined such that: $p(t) = a$ for $0 \leq t \leq 1/a$, and $p(t) = 0$ for $t < 0$ and $t > 1/a$, where a is positive constant. Applying the Laplace transformation to $p(t)$ yields

$$\int_0^\infty p(t)e^{-st}\,dt = \int_0^{1/a} ae^{-st}\,dt = \frac{1 - e^{-s/a}}{s/a} \tag{2.40}$$

Expanding the exponential term as an infinite series, we obtain

$$\frac{1 - e^{s/a}}{s/a} = \frac{1 - [1 - s/a + (s/a)^2/2 + \cdots]}{s/a} = 1 + (s/a) + \cdots \tag{2.41}$$

Now, if $a \to \infty$, then $p(t) \to \delta(t)$, and Equation (2.40) will yield the Laplace transform of $\delta(t)$:

$$\int_0^\infty \delta(t)e^{-st}\,dt = 1 \tag{2.42}$$

Thus, when $X(s) = 1$, the inverse Laplace transformation of $Y(s) = H(s)$ yields the result $y(t) = h(t)$. The system output resulting from the unit impulse input, i.e., the system *impulse response* $h(t)$, is also the inverse Laplace transform of the transfer function $H(s)$.

In the case where $H(s)$ is a known transfer function and $X(s)$ is the Laplace transform of some arbitrary input $x(t)$, we have shown through the example described in Equation (2.38) and Equation (2.39) that the corresponding output $y(t)$ is deduced by performing the inverse Laplace transformation of $Y(s) = H(s)X(s)$. In general, for any $H(s)$ and $X(s)$, we have

$$\begin{aligned} y(t) &= \mathcal{L}^{-1}[H(s)X(s)] = \frac{1}{2\pi j}\int_{\sigma-j\infty}^{\sigma+j\infty} H(s)X(s)e^{st}\,ds \\ &= \frac{1}{2\pi j}\int_{\sigma-j\infty}^{\sigma+j\infty}\int_0^\infty h(\tau)e^{-s\tau}\,d\tau \cdot X(s)e^{st}\,ds = \int_0^\infty \frac{1}{2\pi j}\int_{\sigma-j\infty}^{\sigma+j\infty} X(s)e^{s(t-\tau)}\,ds \cdot h(\tau)\,d\tau \end{aligned} \tag{2.43}$$

Note that in Equation (2.43), we have reversed the order of integration so that the outer integral is based on the time-variable τ. Consider the inner integral, which is a contour integral made with respect to the complex variable s. By definition of the inverse Laplace transform,

$$\frac{1}{2\pi j}\int_{\sigma-j\infty}^{\sigma+j\infty} X(s)e^{s(t-\tau)}\,ds = x(t-\tau) \tag{2.44}$$

Thus, Equation (2.43) simplifies to the following:

$$y(t) = \mathcal{L}^{-1}[H(s)X(s)] = \int_0^\infty h(\tau)x(t-\tau)\,d\tau \tag{2.45}$$

The last term in Equation (2.45) represents the *linear convolution* of $h(t)$ and $x(t)$; this could be considered the most important and most fundamental of all mathematical operations in linear systems and signals analysis. Equation (2.45) forms the basis of the following key notions:

- The multiplication operation in the time-domain is equivalent to the convolution operation in the s-domain. Similarly, it can be shown that the convolution operation in the time-domain is equivalent to the multiplication operation in the s-domain.
- The impulse response, $h(t)$, provides a complete characterization of the dynamic behavior of a given linear system; once $h(t)$ is known, the time-response, $y(t)$, of this system to *any* arbitrary input $x(t)$ can be deduced by *convolving* $h(t)$ with $x(t)$.
- Alternatively, the dynamics of a linear system can also be completely characterized in terms of its transfer function, $H(s)$. Once $H(s)$ is known, the Laplace transform of the system response, $Y(s)$, to any arbitrary input can be deduced by *multiplying* $H(s)$ with the Laplace transform of the input, $X(s)$.

These concepts are illustrated in Figure 2.10.

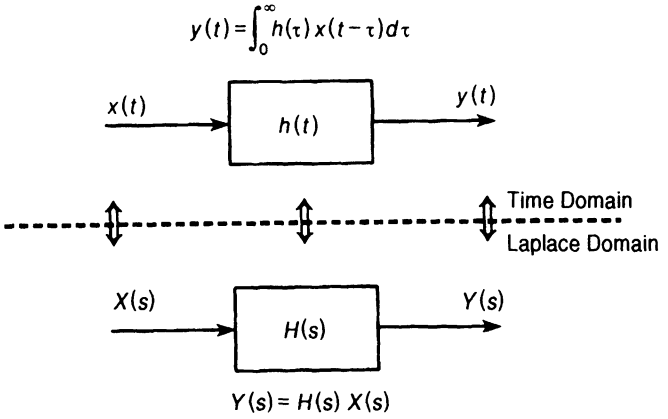

Figure 2.10 The equivalence between block diagram representations in time and Laplace domains.

In the special case where $x(t)$ takes the form of a unit step input (i.e., $x(t) = u(t)$, where $u(t) = 1$ for $t > 0$ and $u(t) = 0$ for $t \leq 0$), Equation (2.45) yields the following result:

$$y(t) = g(t) = \int_0^t h(\tau)\, d\tau \tag{2.46}$$

which implies that the step response, $g(t)$, of a linear system can be obtained by integrating its impulse response with respect to time.

2.8 STATE-SPACE ANALYSIS

To characterize the complexities that are generally found in physiological systems, we often have to resort to the use of differential equations of high order. Analytical solutions of such complicated equations generally are not available, and furthermore, the numerical solution of these high-order differential equations is often fraught with problems of instability. The Laplace transform approach is useful, but this method of solution can become complicated when some of the initial conditions have to assume nonzero values. In such circumstances, *state-space modeling* offers an attractive alternative. A very significant advantage of this approach is that the state-space model can quite easily be extended to characterize *time-varying* and *nonlinear* systems. In addition, problems that are formulated as state-space models are readily amenable to standard parameter estimation techniques, such as Kalman filtering. The use of state-space modeling in system identification (or parameter estimation) is discussed further in Section 7.2.5.

A key premise in state-space analysis is that the dynamics of a given system can be completely characterized by a minimal set of quantities known collectively as the *state*. This means that if the equations describing the system dynamics are known, one can predict the future state of the system given the present state and the complete time-course of the inputs to the system. Suppose we have a linear system that can be described in terms of the following Nth-order differential equation:

$$\frac{d^N y}{dt^N} + a_{N-1}\frac{d^{N-1}y}{dt^{N-1}} + \cdots + a_1\frac{dy}{dt} + a_0 y = b_0 x(t) \tag{2.47}$$

We define a set of N *state variables* $z_1(t), z_2(t), \ldots, z_N(t)$ such that

$$\begin{aligned} z_1(t) &= y(t) \\ z_2(t) &= \frac{dy(t)}{dt} = \frac{dz_1(t)}{dt} \\ &\vdots \\ z_N(t) &= \frac{d^{N-1}y(t)}{dt^{N-1}} = \frac{dz_{N-1}}{dt} \end{aligned} \tag{2.48}$$

Then, using Equation (2.48), we can recast Equation (2.47) into the following form:

$$\frac{dz_N}{dt} = -a_0 z_1 - a_1 z_2 - \cdots - a_{N-1} z_N + b_0 x \tag{2.49}$$

The above equations can be combined to yield the following first-order matrix differential equation:

$$\frac{d\underline{\mathbf{z}}(t)}{dt} = \mathbf{F}\underline{z}(t) + \mathbf{G}x(t) \tag{2.50}$$

where

$$\underline{\mathbf{z}}(t) = \begin{bmatrix} z_1(t) \\ z_2(t) \\ \vdots \\ z_{N-1}(t) \\ z_N(t) \end{bmatrix}, \quad F = \begin{bmatrix} 0 & 1 & 0 & \cdot & \cdot & 0 \\ 0 & 0 & 1 & 0 & \cdot & 0 \\ \vdots & \vdots & \vdots & \vdots & \vdots & \vdots \\ 0 & 0 & 0 & \cdot & 0 & 1 \\ -a_0 & -a_1 & \cdot & \cdot & -a_{N-2} & -a_{N-1} \end{bmatrix} \quad \text{and} \quad G = \begin{bmatrix} 0 \\ 0 \\ \vdots \\ 0 \\ b_0 \end{bmatrix} \tag{2.51}$$

It is clear that, basically, what the state-space approach does is to convert the high-order differential equation (Equation (2.48)) into a set of N first-order differential equations (Equation (2.50)).

Finally, we can relate the state vector $\underline{\mathbf{z}}(t)$ to the output $y(t)$ of the system in question through

$$y(t) = \mathbf{C}\underline{\mathbf{z}}(t) + Dx(t) \tag{2.52}$$

where, in this case,

$$\mathbf{C} = [1 \quad 0 \quad \cdots \quad 0 \quad 0] \qquad \text{and} \qquad D = 0 \tag{2.53}$$

Equation (2.52) allows for the possibility that one might not be able to measure the state variables directly, although in the particular example that we have considered, we are able to observe the first state variable, $z_1(t)$. Equation (2.52) is commonly referred to as the *observation equation*, while Equation (2.50) is called the *state equation*.

In linear systems, it is a relatively simple matter to convert a model represented as a transfer function (i.e., in Laplace transform description) into the state-space form, and vice versa. For the sake of illustration, consider the transfer function given by Equation (2.37b).

We define a new intermediate variable, $U(s)$, such that this transfer function, $H(s)$, can be expressed as the product of two components:

$$H(s) = \frac{U(s)}{X(s)}\frac{Y(s)}{U(s)} = \frac{1}{a_2 s^2 + a_1 s + 1}\frac{b_2 s^2 + b_1 s + b_0}{1} \tag{2.54}$$

Now, the first component of this product yields

$$a_2 s^2 U(s) + a_1 s U(s) + U(s) = X(s) \tag{2.55}$$

The inverse Laplace transform of Equation (2.55) is

$$a_2 \frac{d^2u(t)}{dt^2} + a_1 \frac{du(t)}{dt} + u(t) = x(t) \tag{2.56}$$

As in Equation (2.48), we define the state variables $z_1(t)$ and $z_2(t)$ such that

$$z_1(t) = u(t), \qquad z_2(t) = \frac{dz_1(t)}{dt} = \frac{du(t)}{dt} \tag{2.57}$$

Then, Equation (2.56) can be rewritten

$$\frac{dz_2(t)}{dt} = -\frac{a_1}{a_2} z_2(t) - \frac{1}{a_2} z_1(t) + x(t) \tag{2.58}$$

Equations (2.48) and (2.49) can be combined to form the following matrix state equation:

$$\begin{bmatrix} \frac{dz_1(t)}{dt} \\ \frac{dz_2(t)}{dt} \end{bmatrix} = \begin{bmatrix} 0 & 1 \\ -\frac{1}{a_2} & -\frac{a_1}{a_2} \end{bmatrix} \begin{bmatrix} z_1(t) \\ z_2(t) \end{bmatrix} + \begin{bmatrix} 0 \\ 1 \end{bmatrix} x(t) \tag{2.59}$$

We turn next to the other component of $H(s)$. Here, we have

$$Y(s) = b_2 s^2 U(s) + b_1 s U(s) + b_0 U(s) \tag{2.60}$$

Taking the inverse Laplace transform of Equation (2.60), we obtain

$$y(t) = b_2 \frac{d^2u(t)}{dt^2} + b_1 \frac{du(t)}{dt} + b_0 u(t) \tag{2.61}$$

Then, using Equations (2.57) and (2.58), we obtain the following result:

$$y(t) = \begin{bmatrix} \left(b_0 - \frac{b_2}{a_2}\right) & \left(b_1 - b_2 \frac{a_1}{a_2}\right) \end{bmatrix} \begin{bmatrix} z_1 \\ z_2 \end{bmatrix} + b_2 x(t) \tag{2.62}$$

Thus, conversion of the transfer function in Equation (2.37b) into state-space form leads to the state equation given by Equation (2.59) and the observation given by Equation (2.62).

2.9 COMPUTER ANALYSIS AND SIMULATION—MATLAB AND SIMULINK

Although the use of Laplace transforms and state-space modeling greatly simplifies the mathematical characterization of linear systems, models that provide adequate representations of realistic dynamical behavior are generally too complicated to deal with analytically. In such complex situations, the logical approach is to translate the system block representation into a computer model and to solve the corresponding problem numerically. Traditionally, one

would derive the differential equations that represent the model and develop a program in some basic programming language, e.g., C or Fortran, to solve these equations. However, a variety of software tools are available that further simplify the task of model simulation and analysis. One of these, named SIMULINK®, is currently used by a large segment of the scientific and engineering community. SIMULINK provides a graphical environment that allows the user to easily convert a block diagram into a network of blocks of mathematical functions. It runs within the interactive, command-based environment called MATLAB®. In the discussions that follow, it is assumed that the reader has access to, at least, the Student Versions of MATLAB and SIMULINK, both of which are products of The Mathworks, Inc. (Natick, MA). We also assume that the reader is familiar with the most basic functions in MATLAB. One advantage of employing MATLAB and SIMULINK is that these tools are platform independent; thus, the same commands apply whether one is using SIMULINK on a Windows-based machine or on a Unix-based computer. In the rest of this section, our aim is to give the reader a brief "hands-on" tutorial on the use of SIMULINK by demonstrating in a step-by-step manner how one would go about simulating the linear lung mechanics model discussed in Section 2.3. For more details and advanced topics, the reader is referred to the User's Guides of both SIMULINK (Dabney and Harman, 1998) and MATLAB (Hanselman and Littlefield, 1998).

Let us suppose that we would like to find out how much tidal volume is delivered to a patient in the intensive care unit when the peak pressure of a ventilator is set at a prescribed level. Obviously, the solution of this problem requires a knowledge of the patient's lung mechanics. We assume that this patient has relatively normal mechanics, and the values of the various pulmonary parameters are as follows: $R_C = 1\,\text{cm}\,H_2O\,\text{s}\,L^{-1}$, $R_P = 0.5$ $\text{cm}\,H_2O\,\text{s}\,L^{-1}$, $C_L = 0.2\,L\,\text{cm}\,H_2O^{-1}$, $C_W = 0.2\,L\,\text{cm}\,H_2O^{-1}$, and $C_S = 0.005\,L\,\text{cm}\,H_2O^{-1}$ (see Figure 2.6). We will consider two ways of approaching this problem. The first and most straightforward method is to derive the transfer function for the overall system and use it as a single "block" in the SIMULINK program. The differential equation relating total airflow, Q, to the applied pressure at the airway opening, P_{ao}, was derived using Kirchhoff's laws and presented in Equation (2.16). Substituting the above parameter values into this differential equation and taking its Laplace transform yields, after some rearrangement of terms, the following expression:

$$\frac{Q(s)}{P_{ao}(s)} = \frac{s^2 + 420s}{s^2 + 620s + 4000} \tag{2.63}$$

To implement the above model, run SIMULINK from within the MATLAB command window (i.e., type `simulink` at the MATLAB prompt). The SIMULINK main block library will be displayed in a new window. Next, click the File menu and select `New`. This will open another window named `Untitled`—this is the working window in which we will build our model. The main SIMULINK menu displays several libraries of standard block functions that we can select from for model development. In our case, we would like to choose a block that represents the transfer function shown in Equation (2.63). Open the `Linear Library` (by double-clicking this block): this will open a new window containing a number of block functions in this library. Select `Transfer Fcn` and drag this block into the working window. Double-click this block to input the parameters of the transfer function. Enter the coefficients of the polynomials in s in the numerator and denominator of the transfer function in the form of a row vector in each case. Thus, for our example, the coefficients for the numerator will be [1 420 0]. These coefficients are ordered in descending powers of s. Note that, even

though the constant term does not appear in the numerator of Equation (2.63), it is still necessary to include explicitly as zero the "coefficient" corresponding to this term. Once the transfer function block has been set up, the next step is to include a generating source for P_{ao}. This can be found in the `Sources` library. In our case, we will select and drag the `sine wave` function generator into the working window. Double-click this icon in order to modify the amplitude and frequency of the `sine wave`: we will set the amplitude to 2.5 cm H_2O (i.e., peak-to-peak swings in P_{ao} will be 5 cm H_2O), and the frequency to 1.57 radians s^{-1}. which corresponds to $1.57/(2 \cdot \pi) = 0.25$ Hz or 15 breaths min^{-1}. Connect the output port of the sine wave block to the input port of the transfer function block with a line. To view the resulting output Q, open the `Sinks` library and drag a `Scope` block into the working window. Double-click the `Scope` block and enter the ranges of the horizontal (time) and vertical axes. It is always useful to view the input simultaneously. So, drag another `Scope` block into the working window and connect the input of this block to the line that "transmits" P_{ao}. At this point, the model is complete, and one can proceed to run the simulation. However, it is useful to add a couple of features. We would also like to view the results in terms of volume delivered to the patient. This is achieved by integrating Q. From the `Linear library`, select the `integrator` block. Send Q into the input of this block and direct the output (Vol) of the block to a third `Scope`. It is also advisable to save the results of each simulation run into a data file that can be examined later. From the `Sinks` library, select and drag the `To File` block into the working window. This output file will contain a matrix of numbers. A name has to be assigned to this output file as well as the matrix variable. In our case, we have chosen to give the file the name `respm1.mat`, and the matrix variable the name `respm1`. Note that `mat` files are the standard (binary) format in which MATLAB variables and results are saved. The first row of matrix `respm1` will contain the times that correspond to each iteration step of the simulation procedure. In our case, we would like to save the time-histories of P_{ao}, Q and Vol. Thus, the `To File` block will have to be adjusted to accomodate three inputs. Since this block expects the input to be in the form of a vector, the three scalar variables will have to be transformed into a 3-element vector prior to being sent to the `To File` block. This is achieved with the use of the `Mux` block, found in the `Connections` library. After dragging it into the working window, double-click the `Mux` block and enter 3 for the number of inputs. Upon exiting the `Mux` dialog block, note that there are now three input ports on the `Mux` block. Connect the `Mux` output with the input of the `To File` block. Connect the input ports of the `Mux` block to P_{ao}, Q and Vol. The block diagram of the completed SIMULINK model is shown in Figure 2.11a. The final step is to run the simulation. Go to the `Simulation` menu and select `Parameters`. This allows the user to specify the duration over which the simulation will be conducted, as well as the minimum and maximum step sizes for each computational step. The latter will depend on the dynamics of the system in question—in our case, we have chosen both time-steps to be 0.01 s. The user can also select the algorithm for performing integration. Again, the particular choice depends on the problem at hand. For linear systems, `Linsim` is the most appropriate algorithm. However, `Linsim` should not be used for problems involving nonlinearities. For problems that involve vastly different time-constants, the `Gear` or `Adams/Gear` algorithms may be preferable. The user is encouraged to experiment with different algorithms for a given problem. Some algorithms may produce numerically unstable solutions, while others may not. Finally, double-click `Start` in the `Simulation` menu to proceed with the simulation.

In the SIMULINK model of Figure 2.11a, the bulk of our effort in solving the problem was expended on deriving the analytical expression for the transfer function $Q(s)/P_{ao}(s)$ (Equation (2.16)). This clearly is not the approach that we would want to take in general, since

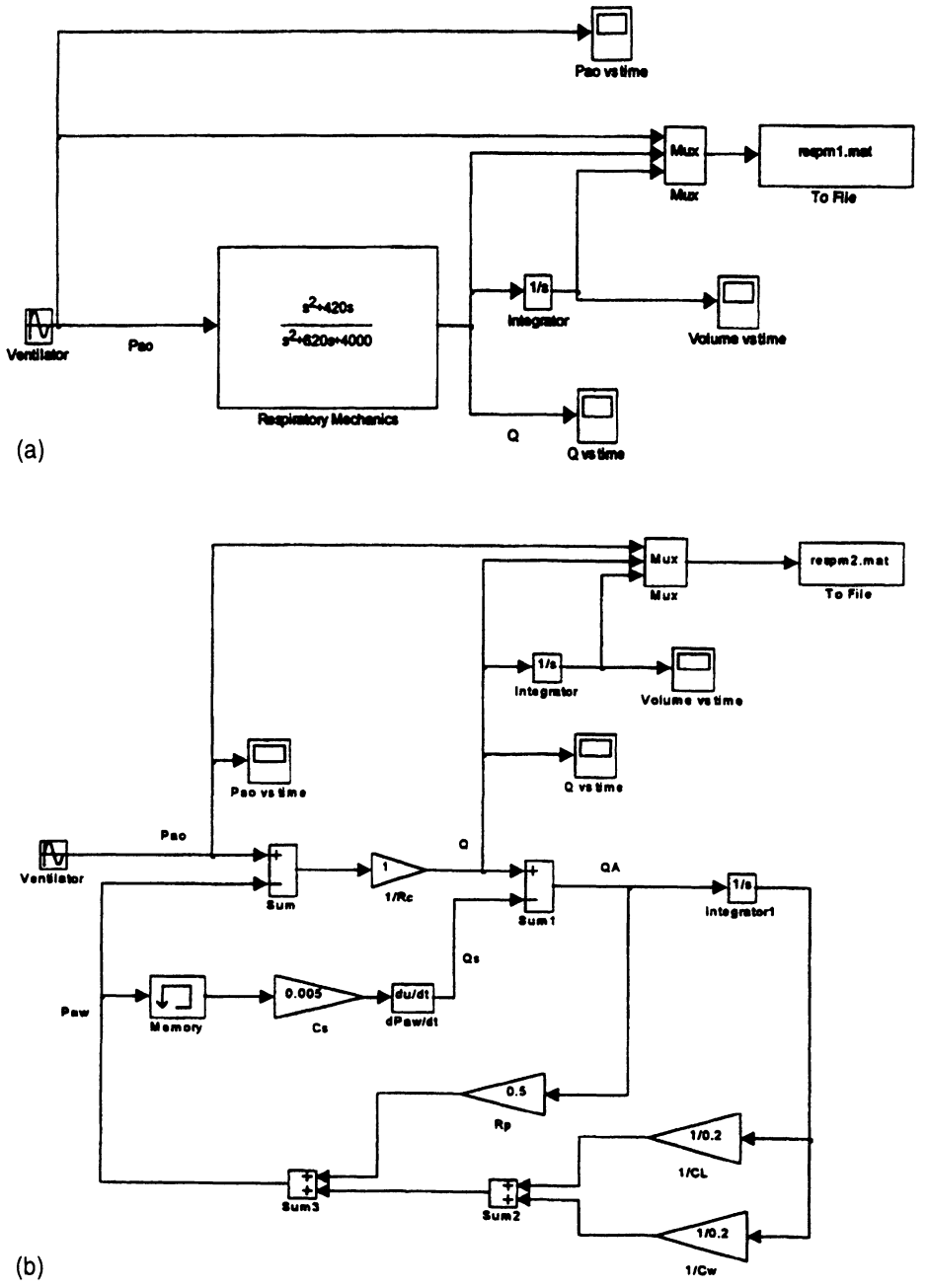

Figure 2.11 Two SIMULINK models of simple lung mechanics.

one of the reasons for computer simulation is to simplify the task of modeling. Obtaining the solution for $Q(t)$, for given P_{ao} and lung mechanical parameters, leads also to the simultaneous solution of other "internal" variables that might be of interest. These include the alveolar pressure, P_A, and the airflow actually delivered to the alveoli, Q_A. However, the implementation of the model in Figure 2.11a does not allow access to these internal variables since the system dynamics are "lumped" into a single transfer function block. The SIMULINK implementation of the same model in Figure 2.11b displays a more "open structure." Various segments in the block diagram shown correspond directly with the basic circuit equations (Equations (2.14) and (2.15)) derived from applying Kirchhoff's laws to the model of Figure 2.6. For instance, the double loop containing the gains $1/C_L$, $1/C_W$, R_P and C_S in the SIMULINK diagram of Figure 2.11b represents Equation (2.14). This kind of open architecture also makes it easier to determine how alterations in the parameters, such as what might occur with different lung diseases, are expected to affect overall lung mechanics. However, a common limitation with this approach is the creation of *algebraic loops*. This problem arises when blocks with direct feedthrough are connected together in a loop. For example, in Figure 2.11b, the gains R_P and C_S are connected together with the derivative block in a closed loop. These functions are all feedthrough blocks, so that at any integration step, the simultaneous solution of the two equations represented by this loop is required. This is accomplished iteratively, but numerical ill-conditioning could lead to no convergent solution. For each algebraic loop, SIMULINK reports an error when more than 200 iterations are expended per integration step. We eliminate this problem in our example by adding a

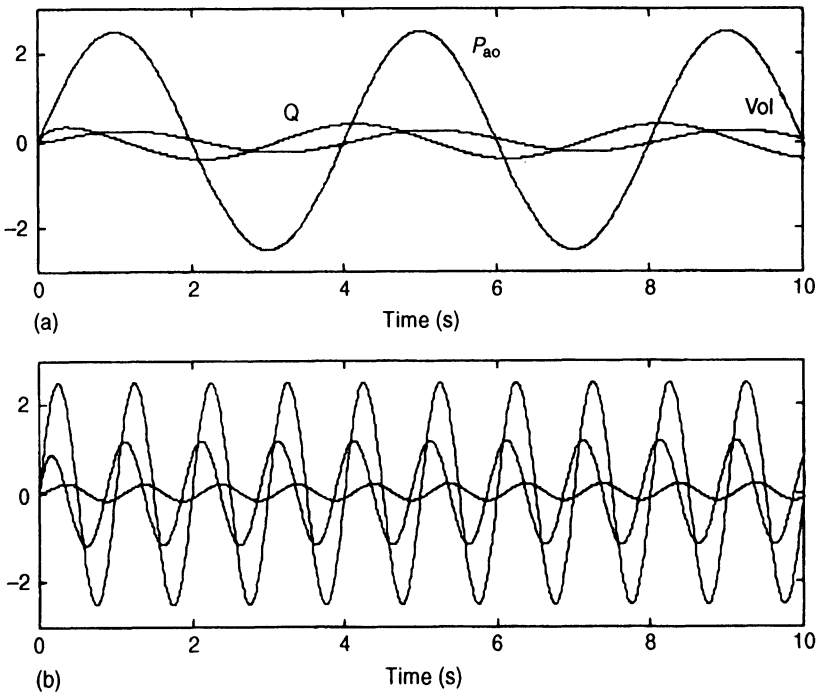

Figure 2.12 Sample simulation results from SIMULINK implementation of lung mechanics model. (a) Predicted dynamics of airflow, Q, and volume, Vol, in response to sinusoidal forcing of P_{ao} (amplitude = 2.5 cm H_2O) at 15 breaths min^{-1}. (b) Predicted dynamics of Q and Vol in response to sinusoidal forcing of P_{ao} (amplitude = 2.5 cm H_2O) at 60 breaths min^{-1}.

`memory` block to the closed loop in question. The `memory` block simply adds a delay of one integration time-step to the circuit. However, one should be cautioned that this "fix" does not always work and, under certain circumstances, could lead to numerical instability.

Figure 2.12 shows sample simulation results produced by either of the model implementations. As indicated earlier, we assume the ventilator generates a sinusoidal P_{ao} waveform of amplitude 2.5 cm H_2O. In Figure 2.12a, the ventilator frequency is set at 15 breaths min^{-1}, which is approximately the normal frequency of breathing at rest. At this relatively low frequency, the volume waveform is more in phase with P_{ao}; the airflow, Q, shows a substantial phase lead relative to P_{ao}. This demonstrates that lung mechanics is dominated by compliance effects at such low frequencies. The peak-to-peak change in volume (i.e., tidal volume) is approximately 0.5 L, while peak Q is $\sim 0.4\,L\,s^{-1}$. When the ventilator frequency is increased fourfold to 60 breaths min^{-1} with amplitude kept unchanged, peak Q clearly increases (to $\sim 1.2\,L\,s^{-1}$), while tidal volume is decreased (to $\sim$0.4 L). Now, Q has become more in phase with P_{ao} while volume displays a significant lag. Thus, resistive effects have become more dominant at the higher frequency. The changes in peak Q and tidal volume with frequency demonstrate the phenomenon pulmonologists refer to as *frequency dependence* of pulmonary resistance and compliance, i.e., the lungs appear stiffer and less resistive as frequency increases from resting breathing.

The SIMULINK programs displayed in Figure 2.11a and Figure 2.11b have been saved as the model files `respm1.mdl` and `respm2.mdl`, respectively. These have been included in the library of MATLAB script files ("m-files") and SIMULINK model files ("mdl-files") accompanying this book. For a full compilation of all script files, model files, and MATLAB and SIMULINK functions employed in this book, the reader is referred to Appendix II.

BIBLIOGRAPHY

Blesser, W.B. *A Systems Approach to Biomedicine*. McGraw-Hill, New York, 1969.

Carlson, G.E. *Signal and Linear System Analysis*, 2d ed. Wiley, New York, 1998.

Dabney, J.B., and T.L. Harman. *The Student Edition of SIMULINK: Dynamic Simulation for MATLAB*. Prentice-Hall, Upper Saddle River, NJ, 1998.

Hanselman, D., and B. Littlefield. *The Student Edition of MATLAB: Version 5, User's Guide*. Prentice-Hall, Upper Saddle River, NJ, 1998.

Milsum, J.H. *Biological Control Systems Analysis*. McGraw-Hill, New York, 1966.

PROBLEMS

P2.1. Develop the mechanical equivalent of the electrical analog of respiratory mechanics shown in Figure 2.6.

P2.2. Develop the electrical analog of the muscle mechanics model shown in Figure 2.7.

P2.3. In emphysematous lungs, the peripheral airways of the diseased regions develop a very high resistance to airflow, and the destruction of the alveolar walls leads to an increased regional compliance. Extend the linear respiratory mechanics model of Figure 2.6 to include a normal and a diseased peripheral lung region, each with its own peripheral resistance and alveolar compliance. Show the electrical analog of the extended model and derive the differential equation relating the airway opening pressure, P_{ao}, to the total airflow, Q, entering the model. Finally, obtain an expression for the transfer function of the model, with P_{ao} as input and Q as output.

P2.4. Figure P2.1 shows a schematic diagram of the 5-element Windkessel model that has been used to approximate the hemodynamic properties of the arterial tree. The model consists of a distensible (as illustrated by the two-ended arrows) aorta and a lumped representation of the rest of the arterial vasculature. The latter is modeled as a simple parallel combination of peripheral resistance, R_P, and peripheral compliance, C_P. The mechanical parameters pertinent to the aortic portion are: (a) the compliance of the aortic wall, C_{ao}, (b) the viscous resistance of the aortic wall, R_{ao}; and (c) the inertance to flow through the aorta, L_{ao}. Note that resistance to flow in the aorta is considered negligible compared to R_P. Construct the electrical analog of this model and derive the transfer function and equivalent state-space model relating aortic pressure, P_{ao}, to aortic flow, Q.

P2.5. A somewhat different version of linear muscle mechanics from that displayed in Figure 2.7 is shown in Figure P2.2. Here, the elastic element, C_P, is placed in parallel to the viscous damping element R and the contractile element, and the entire parallel combination is placed in series with the elastic element, C_S, and the lumped representation of the muscle mass, m. Derive an expression for the transfer function relating the extension of the muscle, x, to an applied force, F. Convert this transfer function description into the equivalent state-space model.

P2.6. Figure P2.3 displays the equivalent circuit of a short length of squid axon according to the Hodgkin–Huxley model of neuronal electrical activity. The elements shown as circles represent voltage sources that correspond to the Nernst potentials for sodium, potassium, and chloride ions. The resistances are inversely proportional to the corresponding membrane conductances for these three types of ions, while C represents membrane capacitance. Derive the Hodgkin–Huxley equation, i.e., the differential equation that relates the net current flowing through the membrane, I, to the applied voltage across the membrane, V.

P2.7. Let us suppose we know that the response of a mechanoreceptor to stretch, applied in the form of a step of magnitude x_0 (in arbitrary length units), is

$$V = x_0(1 - e^{-5t})$$

where the receptor potential, V, is given in millivolts and time from the start of the step, t, is given in seconds. If we assume this system to be linear, deduce an expression for the receptor potential that we would expect to measure in response to the following stretch

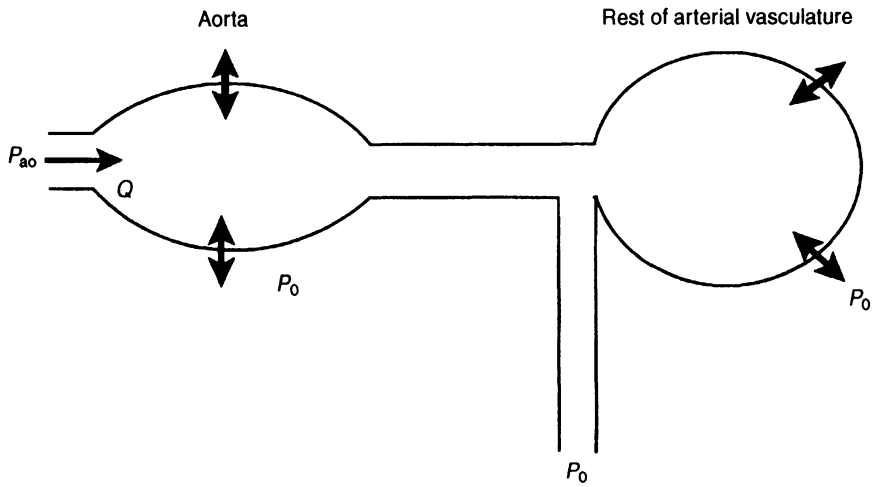

Figure P2.1 Schematic representation of the 5-element Windkessel model of aortic and arterial hemodynamics.

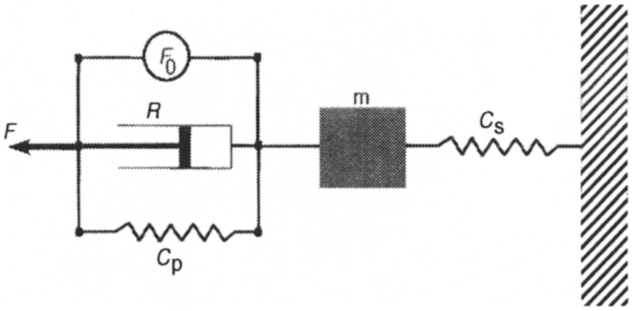

Figure P2.2 Alternative model of muscle mechanics that includes the effect of muscle mass.

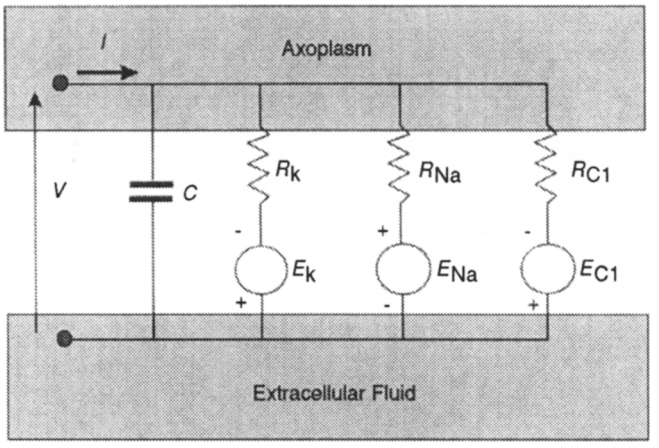

Figure P2.3 Hodgkin–Huxley model of the electrical properties of nerve membrane.

waveform: $x(t) = 0$, $t < 0$; $x(t) = 4$, $0 \leq t < 0.3$; $x(t) = 9$, $0.3 \leq t < 0.8$; $x(t) = 0$, $t \geq 0.8$.

P2.8. Using Laplace transforms, determine the responses of the mechanoreceptor in Problem P2.7 to a unit impulse and a unit ramp (i.e., $x(t) = t$ for $t > 0$).

P2.9. Using the SIMULINK program `respm2.mdl` as the starting point, incorporate into the respiratory mechanics model the effect of inertance to gas flow in the central airways (L_C). Assume a value of 0.01 cm $H_2O\,s^2\,L^{-1}$ for L_C. Keep the values of the other parameters unchanged. Through model simulations, determine how airflow and tidal volume would vary in response to sinusoidal pressure waveforms at the airway opening (P_{ao}) applied at 15, 60, 120, 240, 480, and 960 breaths min^{-1}. To simulate a subject with emphysema, increase lung compliance (C_L) to 0.4 L cm H_2O^{-1} and peripheral airway resistance (R_P) to 7.5 cm $H_2O\,s\,L^{-1}$. Repeat the simulations at the frequencies listed above. Compare the frequency dependence of the resulting airflow and volume waveforms to those obtained for the normal subject.